

# Basic Ray Tracing

Rick Aster and Sue Bilek

October 3, 2003

A key observation that we can make about a seismic signal is its *arrival time*. From systematic observations of arrival times, we can deduce useful properties (e.g., velocity or attenuation) in the Earth. Indeed, much of the early history of seismology, (when the discovery of the Earth's core and many other key results were made) was based almost entirely on arrival time observations. We can understand many arrival time observations with *ray theory*, which describes how short-wavelength seismic energy propagates, where by “short” we mean short relative to any scale lengths in the structure (not counting abrupt jumps in properties). Rays are defined as the normals to the wavefront, so they point in the direction of propagation. Ray theory modeling is considerably easier than solving the wave equation in complex structures. We will restrict our development here to the useful and tractable case of ray behavior in media with seismic velocities varying in only one direction,  $z$ .

Recalling Snell's Law, we note that for a laterally homogeneous Earth where velocity,  $v(z)$  increases with depth (as it does over most of the Earth), seismic rays will be bent more and more towards the horizontal as they travel deeper (Figure 1), so that the horizontal slowness

$$p = \frac{\sin \theta(z)}{v(z)} \quad (1)$$

is conserved everywhere along the ray path, where  $\theta$  is the incidence angle. The incidence angle at the surface is thus

$$\theta(0) = \sin^{-1}(pv(0)) . \quad (2)$$

When the ray is traveling horizontally, we are at the *turning point* depth,  $z_{tp}$  and  $v(z_{tp}) = 1/p$ . Note that an array of seismometers at the surface of the Earth can thus measure the horizontal slowness of a ray and tell what velocity it turned at, if the medium can be adequately approximated by a flat-lying structure and we are examining approximately plane waves.

At any point along a ray, we can express the ray in terms of its horizontal and vertical slownesses (Figure 2),  $p$  and

$$\eta = \frac{\cos \theta(z)}{v(z)} = \sqrt{v^{-2}(z) - p^2} , \quad (3)$$

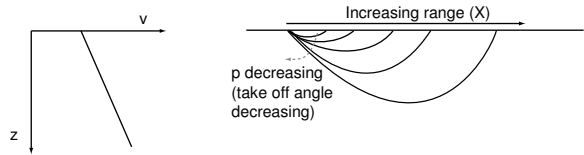


Figure 1: Rays in media of increasing velocity with depth. Generally X increases as p decreases.

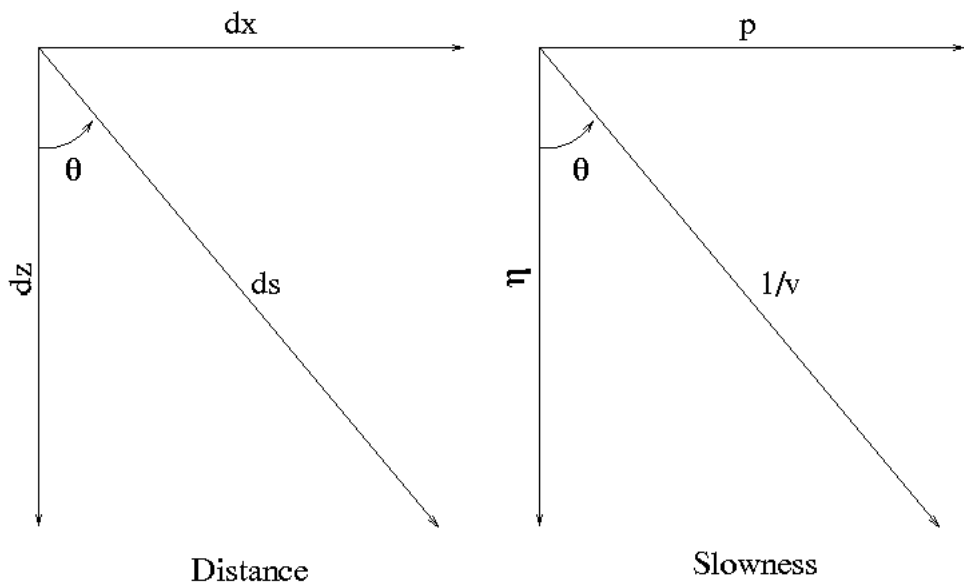


Figure 2: An Infinitesimal Ray Segment

respectively, so that  $p = 1/v$  and  $\eta = 0$  at  $z_{tp}$ .

### Equations for travel time and distance along a ray

For an infinitesimal ray path segment  $ds$  in the  $xz$  plane, we note that

$$\frac{dx}{ds} = \sin \theta = pv \quad (4)$$

and

$$\frac{dz}{ds} = \cos \theta = \eta v = \sqrt{1 - p^2 v^2(z)} \quad (5)$$

so that

$$\frac{dx}{dz} = \frac{dx}{ds} \cdot \frac{ds}{dz} = \frac{p}{\sqrt{v^{-2}(z) - p^2}}. \quad (6)$$

We can thus obtain an integral expression for the horizontal distance traveled by a ray with ray parameter  $p$  between its beginning and its turning point depth,  $z_{tp}$ , as

$$x = p \int_0^{z_{tp}} \frac{dz}{\sqrt{v^{-2}(z) - p^2}} \quad (7)$$

or the total distance traveled from surface-to-surface

$$X(p) = 2p \int_0^{z_{tp}} \frac{dz}{\sqrt{v^{-2}(z) - p^2}}. \quad (8)$$

Similarly the expression for the time of travel is found from  $dt = (1/v)ds$  and

$$\frac{dt}{dz} = \frac{dt}{ds} \cdot \frac{ds}{dz} = \frac{v^{-1}}{\sqrt{1 - p^2 v^2(z)}} \quad (9)$$

to obtain the surface-to-surface travel time

$$T(p) = 2 \int_0^{t_{tp}} \frac{v^{-1}(z) dz}{\sqrt{1 - p^2 v^2(z)}}. \quad (10)$$

These equations are valid for cases where the the velocity is a continuous function of depth.

### Understanding ray trajectories in media with different velocity distributions

To examine how rays propagate in various situations with respect to the ray parameter, consider the derivative of the distance (Equation 8) with respect to the ray parameter

$$\frac{dX}{dp} = 2 \int_0^{z_{tp}} \frac{dz}{\sqrt{v^{-2}(z) - p^2}} + 2p \frac{d}{dp} \int_0^{z_{tp}} \frac{dz}{\sqrt{v^{-2}(z) - p^2}} \quad (11)$$

setting  $q(z) = v^{-1}(z)$ , substituting  $dz = f(q)dq$ , and integrating the second term by parts gives the following slowness integrals

$$\begin{aligned}
\frac{dX}{dp} &= 2 \int_{q_0}^{q_{tp}} \frac{f(q) dq}{\sqrt{q^2 - p^2}} + 2p \frac{d}{dp} \int_{q_0}^{q_{tp}} \frac{f(q) dq}{\sqrt{q^2 - p^2}} \quad (12) \\
&= 2 \int_{q_0}^{q_{tp}} \frac{f(q) dq}{\sqrt{q^2 - p^2}} + 2p \frac{d}{dp} \left( f(q) \cosh^{-1} \left( \frac{q}{p} \right) \Big|_{q_0}^{q_{tp}} - \int_{q_0}^{q_{tp}} \cosh^{-1} \left( \frac{q}{p} \right) f'(q) dq \right) \\
&= 2 \int_{q_0}^{q_{tp}} \frac{f(q) dq}{\sqrt{q^2 - p^2}} + 2p \frac{d}{dp} \left( -f(q_0) \cosh^{-1} \left( \frac{q_0}{p} \right) - \int_{q_0}^{q_{tp}} \cosh^{-1} \left( \frac{q}{p} \right) f'(q) dq \right) \\
&= 2 \int_{q_0}^{q_{tp}} \frac{f(q) dq}{\sqrt{q^2 - p^2}} + \frac{2q_0 f(q_0)}{\sqrt{q_0^2 - p^2}} + 2 \int_{q_0}^{q_{tp}} \frac{q f'(q) dq}{\sqrt{q^2 - p^2}} \\
&= \frac{2q_0 f(q_0)}{\sqrt{q_0^2 - p^2}} + 2 \int_{q_0}^{q_{tp}} \frac{f(q) + q f'(q) dq}{\sqrt{q^2 - p^2}} .
\end{aligned}$$

Defining the velocity-normalized velocity gradient as

$$\zeta = \frac{1}{v} \cdot \frac{dv}{dz} = -v \frac{dq}{dz} \quad (13)$$

so that, as  $f(q) = dz/dq$ ,

$$qf(q) = -\frac{1}{\zeta} \quad (14)$$

gives us

$$f(q) + qf'(q) = \frac{d}{dq} (qf(q)) = \frac{1}{\zeta^2} \cdot \frac{d\zeta}{dq} . \quad (15)$$

Substituting (15) into (12) and changing the variable of integration back to  $z$  finally gives

$$\frac{dX}{dp} = \frac{-2}{\zeta_0 \sqrt{q_0^2 - p^2}} + 2 \int_0^{z_{tp}} \frac{\frac{d\zeta}{dz} dz}{\zeta^2 \sqrt{q^2 - p^2}} \equiv -Y + Z \quad (16)$$

where

$$\frac{d\zeta}{dz} = -\frac{1}{v^2(z)} \left( \frac{dv}{dz} \right)^2 + \frac{1}{v} \frac{d^2v}{dz^2} . \quad (17)$$

For small changes in  $\zeta$  with  $z$ , the first, negative, term in (16) dominates, and  $dX/dp$  is negative. Thus, if the velocity gradient is not too large, we will have rays with smaller  $p$  (deeper turning rays) propagating to greater  $X$ . This is the normal situation that produces a *prograde* travel-time curve. If  $d\zeta/dz$  is sufficiently large, however,  $dX/dp$  may become positive, resulting in a *retrograde* portion of the travel time curve for some range of  $p$ , where smaller  $p$  rays will arrive at smaller values of  $X$ .

An useful simplifying special case occurs when

$$\frac{d\zeta}{dz} = 0 \quad (18)$$

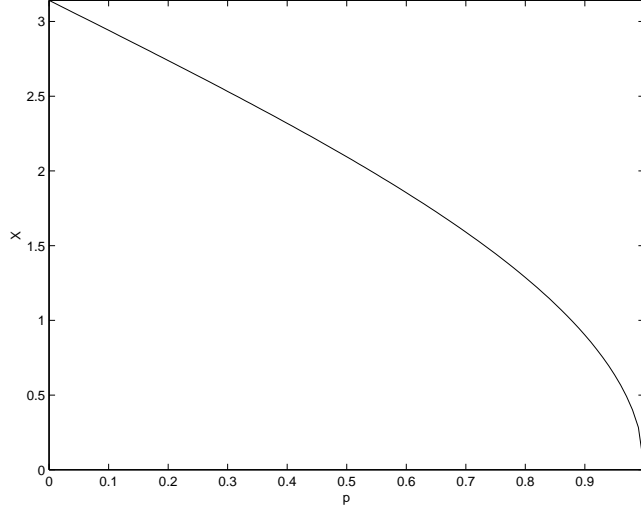


Figure 3:  $X \cdot \alpha$  vs.  $p/v_0$  for a “Normal” Medium.

so that the second term in (16),  $Z$ , is zero. In this case we have

$$\alpha dz = \frac{dv}{v} \quad (19)$$

or

$$v = v_0 e^{\alpha z} \quad (20)$$

which is an exponentially increasing velocity with  $v = v_0$  at  $z = 0$ . For this exponential change in velocity with depth, we can easily integrate (16) to obtain

$$X = \frac{-2}{\alpha} \int_{q_0}^{qtp} \frac{dp}{\sqrt{q_0^2 - p^2}} = \frac{2}{\alpha} \cos^{-1} \left( \frac{qtp}{q_0} \right) = \frac{2}{\alpha} \cos^{-1}(pv_0) . \quad (21)$$

Solving for  $p$  in terms of  $X$  gives

$$p = \frac{dt}{dX} = \frac{1}{v_0} \cos \left( \frac{\alpha X}{2} \right) . \quad (22)$$

Integrating the differential form of  $p$  gives the total travel time

$$T = \frac{2}{\alpha v_0} \sin \left( \frac{\alpha X}{2} \right) . \quad (23)$$

As  $p = dt/dX$  is always positive, travel time always increases with deeper takeoff angles (smaller  $p$ ). In the “normal” case, velocity increases slowly with depth, ( $dv/dz$  and  $d^2v/dz^2$  are small), the  $Y$  term in (16) dominates, and  $dX/dp$  is always negative.  $dX/dp$  has a negative singularity at the surface ( $p = q_0$ ) and

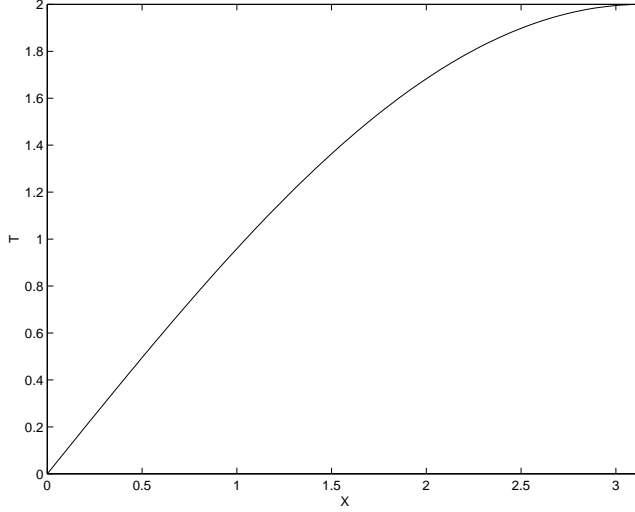


Figure 4:  $T \cdot \alpha \cdot v_0$  vs.  $X \cdot \alpha$  for a “Normal” Medium.

increases monotonically with decreasing  $p$  (Figure 5A). Integrating  $dX/dp$  gives a relationship between  $X$  and  $p$  (Figure 5B). Note that the normal medium gives a finite limiting value of  $X$  at  $p = 0$ , where we would expect an infinite value (Figure(3)). This is a consequence of the unrealistically exponentially increasing velocity for all  $z$ . However, this type of medium will still be a useful approximation for limited  $z$ .

Rotating and reflecting Figure 5B (Figure 5C) and integrating again with respect to  $X$ , gives the travel time curve, which has a monotonically decreasing slope (see also Figure 4).

Next consider a medium with a discontinuous increase in  $dv/dz$  at some depth separating two normal regions (Figure 6), characterized by  $\zeta_1 < \zeta_2$ , which meet where the medium slowness  $q = q_1$ . For rays that turn in the upper layer, the travel time and other behavior is identical to our earlier discussion

$$\frac{dX}{dp} = \frac{-2}{\zeta_1 \sqrt{q_0^2 - p^2}} . \quad (24)$$

For rays that penetrate the lower layer, however, we have

$$\begin{aligned} \frac{dX}{dp} &= \frac{dX_1}{dp} + \frac{dX_2}{dp} \\ &= \frac{-2}{\zeta_1} \left( \frac{1}{\sqrt{q_0^2 - p^2}} - \frac{1}{\sqrt{q_1^2 - p^2}} \right) - \frac{2}{\zeta_2 \sqrt{q_1^2 - p^2}} . \\ &= \frac{-2}{\zeta_1 \sqrt{q_0^2 - p^2}} + \frac{2(\zeta_2 - \zeta_1)}{\zeta_1 \zeta_2 \sqrt{q_1^2 - p^2}} . \end{aligned} \quad (25)$$

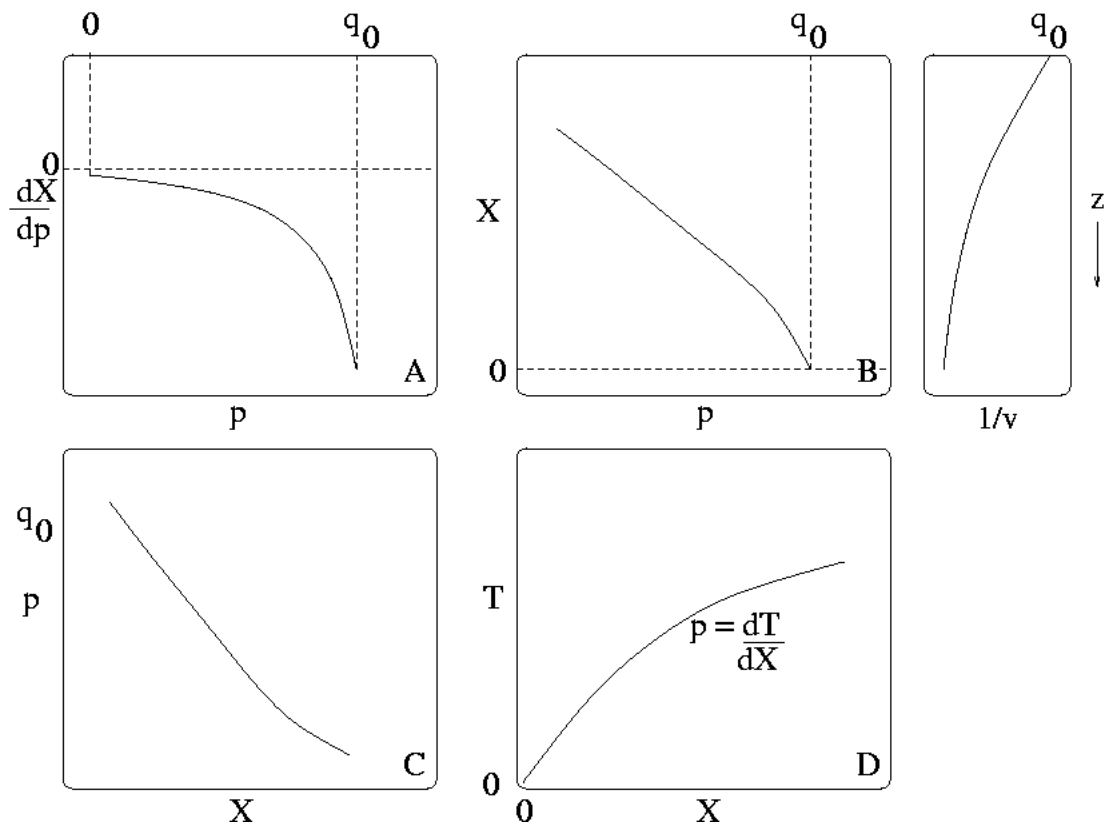


Figure 5: Ray properties for a "Normal" Medium.

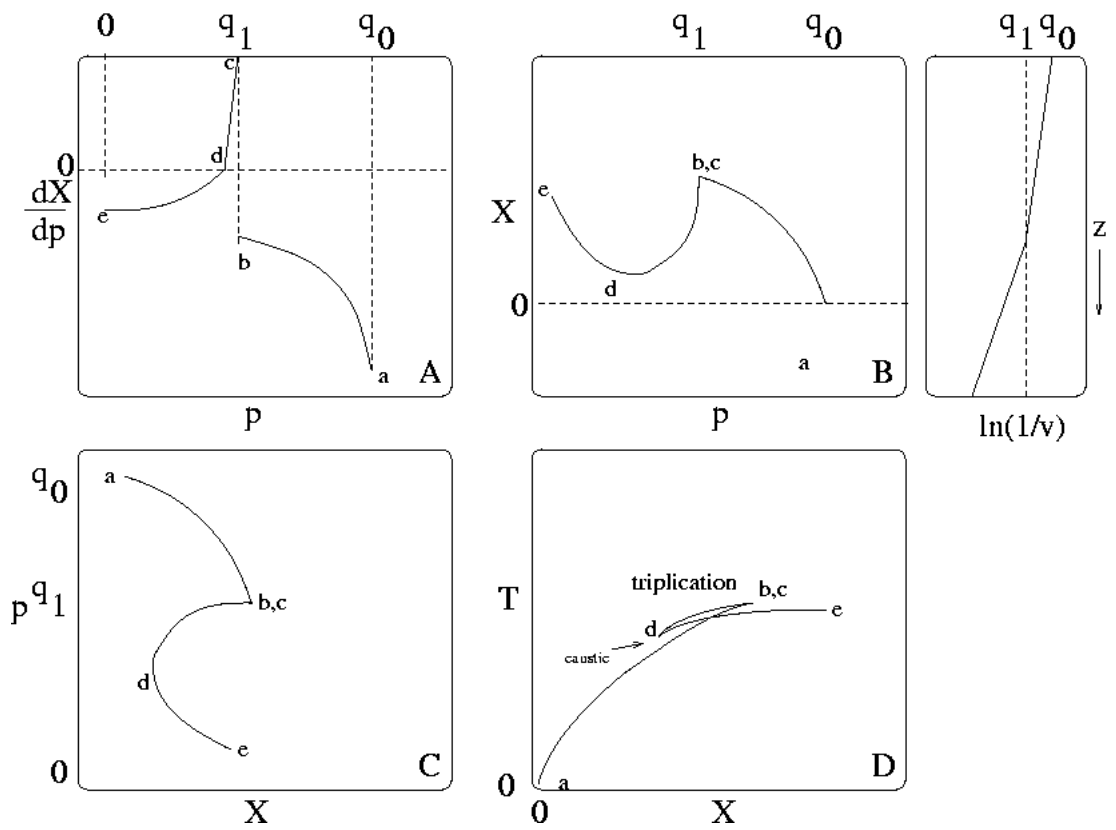


Figure 6: Ray properties for Two-layer Normal Media, Velocity Continuous,  $\zeta_2 > \zeta_1$ .

Figure 6 shows what happens when rays dive into the second layer; a positive singularity occurs in  $dX/dp$  at  $p = q_1$ .  $dX/dp$  also crosses zero to end negative (Figure 6A). Integrating shows that this singularity will introduce a cusp in the  $X$  vs  $p$  curve (Figure 6B, [b,c]), as well as a zero-slope point [d]. Integrating to obtain a travel time curve (Figure 6D) shows that the result is a retrograde portion of the travel-time curve, and hence a region of *triplication* where rays with three different ray parameters all emerge at the same distance, and at different times. This is a basic example of *multipathing*, where there is more than one way for rays to propagate from source to receiver and hence multiple arrivals from a single impulsive source. The distance spanned by the triplication will depend on the magnitude of the gradient discontinuity. At (d),  $dX/dP$  is zero, and rays with ray parameters near the value at (d) will thus tend to focus there. If many ray parameters are excited by a seismic source (say an earthquake or explosion), (d) will be a region where we would expect to see large amplitudes due to ray convergence. Such a point where  $dX/dP$  is zero is called a *caustic*. At point (b,c), on the other hand, we will not have focusing, as  $dX/dP$  is not zero. Instead, we expect vanishingly small amplitudes there from ray convergence, as  $dX/dP$  becomes very large at  $c$ .

Conversely consider the case of a region where velocity decreases with depth (a *low velocity zone* (LVZ)).

For the case of this abrupt velocity decrease, the ray with ray parameter just slightly less than the value where the decrease starts,  $q_1$ , will be refracted downwards into the lower layer and will not turn there until the slowness decreases again to  $q_1$ . The  $dX/dP$  expression is thus

$$\frac{dX}{dp} = \frac{-2}{\zeta_1 \sqrt{q_0^2 - p^2}} . \quad (26)$$

for rays that bottom in the top layer, but becomes

$$\frac{dX}{dp} = \frac{-2}{\zeta_1} \left( \frac{1}{\sqrt{q_0^2 - p^2}} - \frac{1}{\sqrt{q_1^2 - p^2}} \right) - \frac{2}{\zeta_2 \sqrt{q_2^2 - p^2}} . \quad (27)$$

for rays that penetrate the lower layer, where  $q_2 > q_1$  is the slowness at the top of layer 2. There is a discontinuity in the travel-time curve at  $p = q_1$ , where the jump in velocity also introduces a reflected branch. As rays penetrate deeper, the corresponding  $X$  vs.  $p$  curve now has a discontinuous jump from points  $b$  to  $c$  (Figure 7). The travel-time curve eventually becomes normal (prograde) again at (d), but there will always be a *shadow zone* in  $X$  where there are no direct rays. The extent of the shadow zone depends on the thickness and magnitude of the low velocity zone. for the abrupt decrease, there are no caustics (there will be a caustic at (d) for a gradual decrease).

### Rays in a sphere

The equations above assume horizontally layered structure, which is valid using crustal arrivals in the upper 30 km and short distances ( $X < 1000$  km).

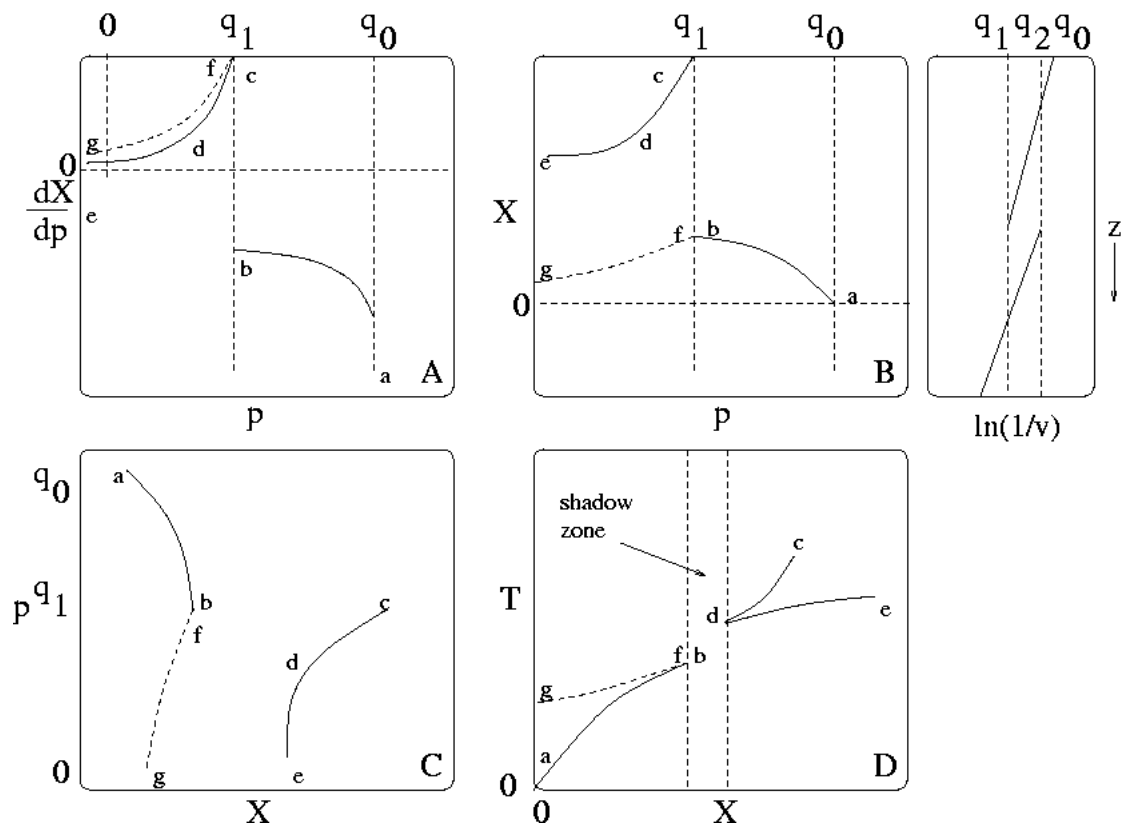


Figure 7: Ray properties for Two-layer Normal Media, Continuous, Region of Abrupt Velocity Decrease

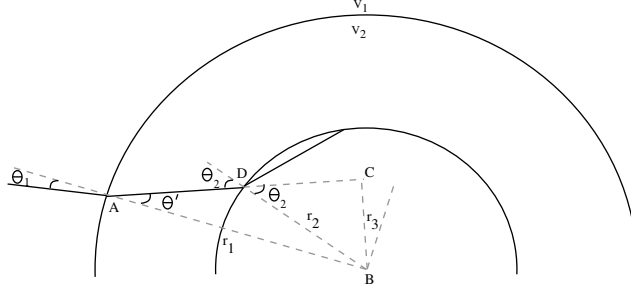


Figure 8: Ray geometry in spherical shells where  $v_1 < v_2$

In order to account for the spherical nature of the Earth, we can modify the definition of  $p$  to reflect the fact that the ray angle from the radius will change along the ray path. Figure 8 shows the geometry for rays traveling through concentric shells of constant velocity.

Using Snell's Law, we see at the interface between shell 1 and shell 2,

$$\frac{\sin \theta_1}{v_1} = \frac{\sin \theta'}{v_2} \quad (28)$$

At the base of layer 2, we can relate the angles  $\theta_1$  to  $\theta_2$  by looking at the geometry of the triangles ABC and DBC. We see that

$$r_2 \sin \theta_2 = r_1 \sin \theta' \quad (29)$$

so that

$$\frac{r_1 \sin \theta_1}{v_1} = \frac{r_2 \sin \theta_2}{v_2} = p \quad (30)$$

Recall that for the flat earth approximation,  $p$  is horizontal slowness with units of (time/distance)

$$p_f = \frac{\sin \theta}{v} = \frac{dt}{dX} \quad (31)$$

For spherical Earth,  $dX = d\Delta r$ , where  $\Delta$  is the angle in radians, so

$$p_s = r \frac{dt}{dX} = \frac{dt}{d\Delta} \quad (32)$$

and has units of time (s/radians).

Returning to the equations for travel time and distance (8 and 10) as described before for the flat Earth, we can write similar expressions for spherical geometry

$$\Delta(p_s) = 2p_s \int_{r_{tp}}^{r_E} \frac{1}{\sqrt{(ur)^2 - p_s^2}} \frac{dr}{r} \quad (33)$$

and

$$T(p_s) = 2 \int_{r_{tp}}^{r_E} \frac{(ur)^2}{\sqrt{(ur)^2 - p_s^2}} \frac{dr}{r} \quad (34)$$

where  $u = 1/v$  and  $r_E$  is the radius of the Earth.

### **Naming of Rays**

Because the Earth has many distinct layers (such as crust, mantle, outer core, inner core), interactions between  $P$  and  $S$  waves and these layers give rise to many possible ray geometries (seismic phases).

#### *Whole earth phases*

$P$ :  $P$  wave in the mantle

$K$ :  $P$  wave in the outer core

$I$ :  $P$  wave in the inner core

$S$ :  $S$  wave in the mantle

$J$ :  $S$  wave in the inner core

$c$ : reflection off the CMB

$i$ : reflection off the inner core boundary

These abbreviations can be used for multiple segments of the raypaths between source and receiver (i.e. PP, PPP, SS, SP). The upgoing branch in surface reflections is denoted by lowercase  $p$  and  $s$ .

#### *Crustal phases*

$Pg$ :  $P$  wave turning within the crust

$PmP$ :  $P$  wave reflecting off the Moho

$Pn$ :  $P$  wave traveling in uppermost mantle below the Moho

Crustal  $S$  waves have similar naming conventions.

### **Using travel time observations**

There is an entire branch of seismology that makes use of travel time data to infer information about the seismic velocity structure (e.g., seismic tomography, or reflection seismology). Travel time curves similar to those in Figures 6, 7 are important for interpreting actual data profiles. Prominent triplications result from the velocity increases at the Moho, near 440 km and 660 km depth in the mantle and lower velocities in the core produce a significant shadow zone (Figure 9).

Some of the first seismic travel time curves and tables were developed by Oldham, Zöpritz, Turner and Gutenberg between 1906 and 1914. This data was used to discover the existence of the core. Travel times were used by Mohorovičić to discover the discontinuity between the crust and mantle in 1909. The first complete velocity models of the interior using travel time data were produced in the 1930's by several seismologists. These models are very similar in general features such as the crust (0-30 km), mantle (30-2900 km) and core (2900-6370 km). The primary differences between the models were in the details near the boundary discontinuities.

The J-B tables, produced by Jeffreys and Bullen in 1940, were the first widely adopted travel time tables and are still used today. For teleseismic distances, these tables can predict travel times of major phases to within a few seconds. Since the 1960's travel times are cataloged by the ISC from seismic stations all over the world and are used to discern Earth structure. The preliminary reference Earth model (PREM) was published in 1981, using body wave travel time

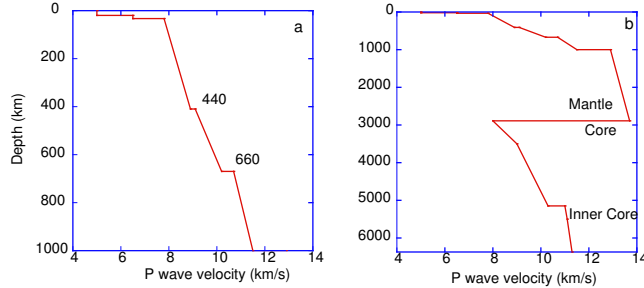


Figure 9: Simple velocity models for the Earth, showing velocity jumps at 440 and 660 km (a), as well as the velocity decrease at the core-mantle boundary (b).

data as well as other seismological and geophysical datasets including surface wave dispersion, and free oscillation data. ISC data was used in the late 1980's early 1990's to produce the *iasp91* velocity model for a spherically symmetric earth. Travel time curves using the *iasp91* velocity model are shown in Figure 10. More recent improvements to the velocity models have come by adding details from the core phases (in model *ak135*), anisotropy, and 3-D structure.

The ray tracing equations described above can be used to compute theoretical travel time curves for radial Earth models. The more difficult problem is the inverse one, producing velocity models derived from the travel time data. In many cases, a 1-D average model is produced using all the available data. This method can have some problems, particularly with the non-uniqueness of models produced with first arrival data, and the errors produced from noise in travel time data.

#### *Seismic tomography*

If there is adequate 3D ray coverage allowing for many crossing raypaths, travel time observations can be used in the seismic tomography problem. Typically this involves using the 1-D model as a reference velocity model and calculating travel time residuals. The residuals are then inverted for velocity differences relative to the 1D model. The travel times are related to the slowness ( $1/v$ ), so any velocity anomaly can also be related to a slowness anomaly

$$\Delta\eta = \frac{1}{v + \Delta v} - \frac{1}{v} \approx -\frac{\Delta v}{v^2}. \quad (35)$$

Travel time residuals  $\Delta t$  can then be related to the slowness (and velocity) anomalies through

$$\Delta t = l\Delta\eta = -\frac{l\Delta v}{v^2} \quad (36)$$

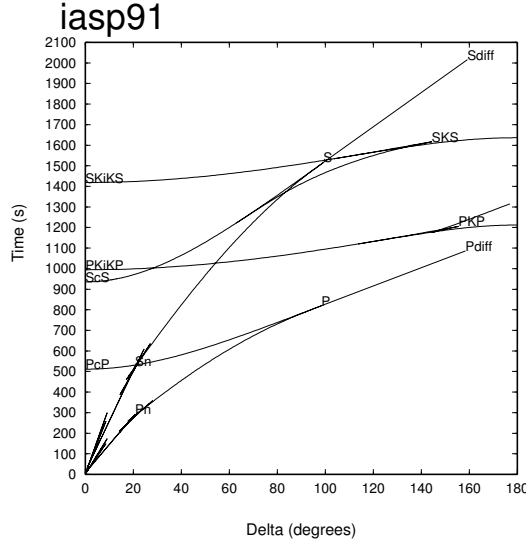


Figure 10: Travel time curves using the isap91 velocity model

where  $l$  is the length of the raypath through the anomalous area. The study region is typically divided up into cells of velocity that differs by  $\Delta v$  from the reference model  $v$ . The travel time residuals at individual stations are then assigned to the sum of time increments in each cell

$$\Delta t = \sum_{i=1}^N \frac{l_i \Delta v_i}{v_i^2} . \quad (37)$$

One ray crosses  $N$  cells and has  $N$  unknowns ( $\Delta v_i$ ). A complete model with multiple rays will have  $M$  cells and  $M$  unknowns ( $\Delta v_i$ ). Because each ray will enter only a limited number of cells ( $N < M$ ), the problem requires many rays crossing each of the cells from different directions (i.e. need a dense array of stations that record seismic waves from many different sources). The  $M$  unknowns can then be solved for using a system of many linear equations, and given the large number of observations needed, complex inversion techniques and statistical methods are used. This is a simplified view of the tomography problem, a nice review of seismic tomography of the lithosphere is given in Thurber, C.H., *Seismic tomography of the lithosphere with body waves*, *Pure and Applied Geophysics*, 160, 717-737, 2003.

#### *Earthquake location*

Travel time data is also important for locating earthquakes. Location information given in standard catalogs, such as the Preliminary Determination of Epicenters, is based on travel times of high frequency body waves. These lo-

cations are solved through a system of linear equations relating the observed travel times and the travel times calculated from an initial hypocenter, with the 4 variables being the three hypocentral coordinates and origin time).